IJE TRANSACTIONS A: Basics Vol. 26, No. 4, (April 2013) 433-446

International Journal of Engineering

Journal Homepage: www.ije.ir

On Symmetric and Asymmetric Buckling Modes of Functionally Graded Annular Plates under Mechanical and Thermal Loads

A. Hasani Baferani*[a], A. R. Saidi [b], A. Naderi [b]

[a] *Department of Mechanical Engineering, Amirkabir University of Technology, Tehran, Iran.*
[b] *Department of Mechanical Engineering, Shahid Bahonar University of Kerman, Kerman, Iran.*

PAPER INFO

Paper history:
Received 29 December 2011
Received in revised form 03 October 2012
Accepted 18 October 2012

Keywords:
Annular Plate
Functionally Graded Material
Buckling
Thermal Buckling
Symmetric and Asymmetric Modes

ABSTRACT

In the present article, buckling analysis of functionally graded annular thin and moderately thick plates under mechanical and thermal loads is investigated. The equilibrium and stability equations of the plate are obtained based on both classical and first order shear deformation plate theories. By using an analytical method, the coupled stability equations are converted to independent equations which can be solved analytically. Solving the decoupled equations and satisfying the boundary conditions yield an eigenvalue problem to find the critical buckling load and/or temperature. Both symmetric and asymmetric modes of buckling and thermal buckling of functionally graded annular plates are investigated. The results show that the buckling mode number may vary with the variation of power law index, annularity and radius-thickness ratio. Finally, the effects of annularity, plate thickness and power law index on buckling load/temperature of functionally graded annular plates are investigated and the buckling mode shapes are plotted.

doi: *10.5829/idosi.ije.2013.26.04a.12*

1. INTRODUCTION

The critical buckling load and/or temperature of the circular and annular plates are significant parameters to design the aeronautical and mechanical structures subjected to in-plane mechanical or thermal loads. It is desirable that the plates are designed at the lowest weight under in-plane loads or high temperature. Annular plates are key components in many structures and machinery applications. For example, they are applied in flight vehicle, power planets, clutch plates, flywheels, brake systems in automotive vehicles and electronic applications such as sensors and micro pumps.

Functionally graded materials (FGM's) are inhomogeneous materials in which the material properties are varied continuously from one point to another point [1-3]. Typically, these materials are made from a mixture of metal and ceramic, or a combination of different metals. They are high performance heat resistant materials which can withstand ultra high temperature and extremely large thermal gradients current in the aerospace industries. The ceramic part of functionally graded (FG) plates provides the high temperature resistance due to its low thermal conductivity and the metal constituent of material resists on the failure of the plate.

Buckling of annular plates was studied firstly by Dean in 1924 [4]. He studied the buckling of a circular annular plate subjected to shearing forces distributed along the edges. Since then, many researchers investigated the buckling of circular annular plates subjected to various loading conditions. In review of recent developments in buckling of homogenous, composite and FG plates a number of investigations have been published in the literatures. Yamaki [5] studied the buckling of a thin annular isotropic plate under uniform compression. An important ramification of his work was that the least buckling load might involve circumferential buckling rather than just axisymmetric modes. Elishakoff and Stavsky [6] studied the axisymmetric buckling of certain annular composite plates. They studied the effect of heterogeneity of plates on the elastic stability of annular plates. Srivinasan and Ramachandra [7] performed the axisymmetric buckling and post buckling of bimodulus annular plates using finite element method. Based on the first order shear

*Corresponding Author Email: a_hasani_baferani@aut.ac.ir (A. Hasani Baferani)

deformation plate theory, Chang [8] studied the axisymmetric buckling of moderately thick polar orthotropic annular plates. Ciancio and Reyes [9] studied buckling of circular annular plates with continuously variable thickness. They used an analytical approach based on the optimized Rayligh-Ritz method. Xu et al. [10] performed axisymmetric buckling of transversely isotropic circular and annular plates. They investigated the general solution of the three-dimensional governing equations for the axisymmetric buckling analysis problem and obtained exact solutions for appropriate boundary conditions. Arfat et al. [11]studied the vibration and buckling of annular and circular plates subjected to a thermal load. They modeled the plate using the dynamic analogue of Saint-Venant plate theory and solved the stability state heat conduction equation for the radial temperature distribution. Ma and Wang [12] studied the relationships between axisymmetric bending and buckling solutions of FG circular plates based on the third-order shear deformation and classical plate theories. Birman and Simitses [13] performed buckling and bending analysis of cylindrically orthotropic annular plates. They presented a closed form solution for arbitrary boundary conditions under mechanical and thermal loads. Najafizadeh and Eslami [14] studied the buckling analysis of thin functionally graded circular plates under uniform radial compression based on the classical plate theory. Also, they [15] studied thermoelastic stability of orthotropic circular plates and obtained closed form solution for buckling temperature of such plates under both clamped and simply supported boundary conditions. Moreover, they investigated thermoelastic stability of functionally graded solid circular plates based on the first order shear deformation theory [16]. Based on the higher order shear deformation theory, Najafizadeh and Heydari performed thermal buckling [17] and mechanical buckling analyses [18] of FG circular plates. Saidi et al. [19] studied the axisymmetric bending and buckling analysis of thick FG circular plates using unconstrained third-order shear deformation plate theory. Naderi and Saidi [20] studied buckling problem of thin FG sector and annular sector plates resting on Winkler and Pasternak elastic foundations. They assumed that the annular sector plate has simply supported straight edges. Also, Naderi and Saidi [21] performed buckling analysis of moderately thick FG sector and annular sector plates based on the first order shear deformation plate theory. They performed similar analysis for sector plates resting on Winkler elastic foundation [22]. Saidi and Hasani Baferani [23] studied thermal buckling problem of FG annular sector plates by using the first order shear deformation plate theory.

Although circular and annular plates geometrically are symmetric structures, the buckling may occur at asymmetric mode shapes. So, both symmetric and asymmetric modes have to be considered for buckling analysis of such plates. To the best of authors' knowledge, buckling problem of FG annular plate subjected to mechanical and/or thermal loads have only been solved by considering the symmetric modes.

In the present article, buckling problem of FG annular plates under in-plane compressive loads and/or temperature is solved based on both symmetric and asymmetric modes. The stability equations are obtained based on both the classical and first order shear deformation theories. Introducing some new functions, the stability equations are decoupled into independent equations which are solved analytically. Both symmetric and asymmetric modes of buckling for functionally graded annular plates under mechanical and thermal loads are investigated. For some special cases, the presented results are compared with those reported in the available papers and a good agreement can be seen. Finally, the effects of annularity, boundary conditions, plate thickness and power law index on the critical buckling load and/or temperature of FG annular plates are discussed in detail.

2. EQUIBLIRIUM EQUATIONS

Consider a FG annular plate with the inner radius a, outer radius b and thickness h, under uniform compressive in-plane load P and/or uniform temperature applied on the inner and outer circular edges (Figure 1). Based on the classical plate theory, the displacement components in the polar coordinate are given by:

$$\begin{aligned} u_r(r,\theta,z) &= u(r,\theta) - z\frac{\partial w(r,\theta)}{\partial r} \\ u_\theta(r,\theta,z) &= v(r,\theta) - \frac{z}{r}\frac{\partial w(r,\theta)}{\partial \theta} \\ u_z(r,\theta,z) &= w(r,\theta) \end{aligned} \quad (1)$$

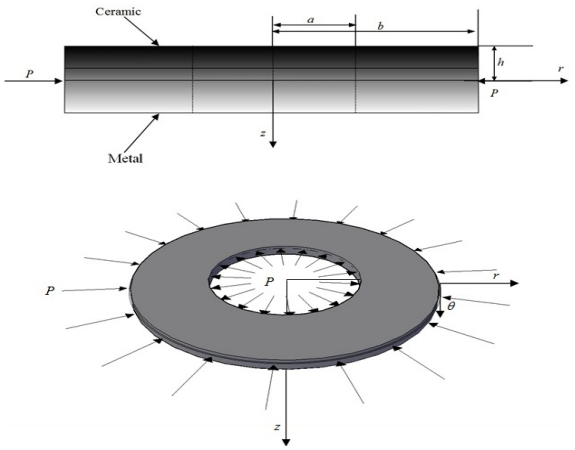

Figure 1. Geometry and coordinate system of FG annular plate under uniform in-plane load

where u, v and w denote the displacements of a point on the middle plane of the plate along r,θ and z directions, respectively. Assuming the large deflection, the strain components of the annular plate can be expressed as:

$$\begin{aligned}
\varepsilon_{rr} &= \frac{\partial u}{\partial r}+\frac{1}{2}(\frac{\partial w}{\partial r})^2 - z\frac{\partial^2 w}{\partial r^2}\\
\varepsilon_{\theta\theta} &= \frac{1}{r}(u+\frac{\partial v}{\partial \theta})+\frac{1}{2r^2}(\frac{\partial w}{\partial \theta})^2 - \frac{z}{r}(\frac{\partial w}{\partial r}+\frac{\partial^2 w}{\partial \theta^2})\\
2\varepsilon_{r\theta} &= \frac{1}{r}\frac{\partial u}{\partial \theta}+\frac{\partial v}{\partial r}-\frac{v}{r}+\frac{1}{r}(\frac{\partial w}{\partial r})(\frac{\partial w}{\partial \theta})\\
&\quad -\frac{2z}{r}(\frac{\partial^2 w}{\partial r\partial \theta}-\frac{1}{r}\frac{\partial w}{\partial \theta})\\
\varepsilon_{rz} &= 0\\
\varepsilon_{\theta z} &= 0
\end{aligned} \tag{2}$$

On the other hand, based on the first order shear deformation plate theory, the displacement components of the plate in r,θ and z directions are assumed to be:

$$\begin{aligned}
u_r(r,\theta,z) &= u(r,\theta)+z\psi_r(r,\theta)\\
u_\theta(r,\theta,z) &= v(r,\theta)+z\psi_\theta(r,\theta)\\
u_z(r,\theta,z) &= w(r,\theta)
\end{aligned} \tag{3}$$

where ψ_r and ψ_θ are the rotation functions of the middle surface. Here, the nonlinear strain components are written in the form of:

$$\begin{aligned}
\varepsilon_{rr} &= \frac{\partial u}{\partial r}+\frac{1}{2}\left(\frac{\partial w}{\partial r}\right)^2+z\frac{\partial \psi_r}{\partial r}\\
\varepsilon_{\theta\theta} &= \frac{1}{r}\left(u+\frac{\partial v}{\partial \theta}\right)+\frac{1}{2r^2}\left(\frac{\partial w}{\partial \theta}\right)^2+\frac{z}{r}\left(\psi_r+\frac{\partial \psi_\theta}{\partial \theta}\right)\\
2\varepsilon_{r\theta} &= \frac{1}{r}\frac{\partial u}{\partial \theta}+\frac{\partial v}{\partial r}-\frac{v}{r}+\frac{1}{r}\left(\frac{\partial w}{\partial r}\right)\left(\frac{\partial w}{\partial \theta}\right)\\
&\quad +z\left(\frac{1}{r}\frac{\partial \psi_r}{\partial \theta}+\frac{\partial \psi_\theta}{\partial r}-\frac{\psi_\theta}{r}\right)\\
2\varepsilon_{rz} &= \frac{\partial w}{\partial r}+\psi_r\\
2\varepsilon_{\theta z} &= \frac{1}{r}\frac{\partial w}{\partial \theta}+\psi_\theta
\end{aligned} \tag{4}$$

The Hooke's law for the FG plate is written as:

$$\begin{aligned}
\sigma_{rr} &= \frac{E(z)}{1-\nu^2}\left(\varepsilon_{rr}+\nu\varepsilon_{\theta\theta}-(1+\nu)\alpha(z)T(r,\theta,z)\right)\\
\sigma_{\theta\theta} &= \frac{E(z)}{1-\nu^2}\left(\varepsilon_{\theta\theta}+\nu\varepsilon_{rr}-(1+\nu)\alpha(z)T(r,\theta,z)\right)\\
\sigma_{r\theta} &= \frac{E(z)}{2(1+\nu)}\left(2\varepsilon_{r\theta}\right)\\
\sigma_{\theta z} &= \frac{E(z)}{2(1+\nu)}\left(2\varepsilon_{\theta z}\right)\\
\sigma_{rz} &= \frac{E(z)}{2(1+\nu)}\left(2\varepsilon_{rz}\right)
\end{aligned} \tag{5}$$

where, ν is the Poisson ratio of the FG plate which is assumed to be a constant and $T(r,\theta,z)$ is the temperature distribution. Also, the parameters $E(z)$ and $\alpha(z)$ are the Young modulus and the coefficient of thermal expansion of the FG plate which vary through the thickness according to the following power law function

$$\begin{aligned}
E(z) &= E_m+(E_c-E_m)\left(\frac{1}{2}-\frac{z}{h}\right)^n\\
\alpha(z) &= \alpha_m+(\alpha_c-\alpha_m)\left(\frac{1}{2}-\frac{z}{h}\right)^n
\end{aligned} \tag{6}$$

where n denotes the power law index which is equal or greater than zero and the subscripts m and c refer to metal and ceramic components, respectively. It is noticeable that in the classical plate theory, the last two relations of Equation (5) are vanished. Using the principle of minimum potential energy, the equilibrium equations for both of the theories can be readily found as [24, 25].

$$\frac{\partial N_{rr}}{\partial r}+\frac{1}{r}\frac{\partial N_{r\theta}}{\partial \theta}+\frac{N_{rr}-N_{\theta\theta}}{r}=0 \tag{7a}$$

$$\frac{\partial N_{r\theta}}{\partial r}+\frac{1}{r}\frac{\partial N_{\theta\theta}}{\partial \theta}+\frac{2N_{r\theta}}{r}=0 \tag{7b}$$

$$\frac{\partial M_{rr}}{\partial r}+\frac{1}{r}\frac{\partial M_{r\theta}}{\partial \theta}+\frac{M_{rr}-M_{\theta\theta}}{r}-Q_r=0 \tag{7c}$$

$$\frac{\partial M_{r\theta}}{\partial r}+\frac{1}{r}\frac{\partial M_{\theta\theta}}{\partial \theta}+\frac{2M_{r\theta}}{r}-Q_\theta=0 \tag{7d}$$

$$\begin{aligned}
&\frac{\partial Q_r}{\partial r}+\frac{1}{r}\frac{\partial Q_\theta}{\partial \theta}+\frac{Q_r}{r}+\frac{1}{r}\frac{\partial}{\partial r}\left(rN_{rr}\frac{\partial w}{\partial r}\right)+\frac{1}{r^2}\frac{\partial}{\partial \theta}\left(N_{\theta\theta}\frac{\partial w}{\partial \theta}\right)\\
&+\frac{2N_{r\theta}}{r}\frac{\partial^2 w}{\partial r\partial \theta}=0
\end{aligned} \tag{7e}$$

where, $N_{rr}, N_{\theta\theta}$ and $N_{r\theta}$ are the in-plane force resultants, $M_{rr}, M_{\theta\theta}$ and $M_{r\theta}$ are the moment resultants defined as:

$$\begin{aligned}
\left(N_{rr},N_{\theta\theta},N_{r\theta}\right) &= \int_{-h/2}^{h/2}\left(\sigma_{rr},\sigma_{\theta\theta},\sigma_{r\theta}\right)dz\\
\left(M_{rr},M_{\theta\theta},M_{r\theta}\right) &= \int_{-h/2}^{h/2}\left(\sigma_{rr},\sigma_{\theta\theta},\sigma_{r\theta}\right)zdz
\end{aligned} \tag{8}$$

and in the first order shear deformation plate theory, the out of plane force resultants, Q_r and Q_θ, are defined as:

$$\left(Q_r,Q_\theta\right)=k^2\int_{-h/2}^{h/2}\left(\sigma_{rz},\sigma_{\theta z}\right)dz \tag{9}$$

where k^2 is the shear correction factor assumed to be $5/6$. It is noticeable that in the classical plate theory by substituting Q_r and Q_θ from Equations (7c) and (7d) into Equation (7e), the bending equation is obtained. In the above equations, the superscript C and F are referred to classical and first order shear deformation theories, respectively.

3. STABILITY EQUATIONS

The stability equations of the plate can be derived from the adjacent equilibrium criterion [26]. For accustom on this method and related equation, the reader can see

Refs. [20-23]. Using the procedure introduced in these references, the stability equation of FG annular plate can be easily derived as:

$$\begin{aligned}
&\frac{\partial N_{rr1}}{\partial r}+\frac{1}{r}\frac{\partial N_{r\theta 1}}{\partial \theta}+\frac{N_{rr1}-N_{\theta\theta 1}}{r}=0\\
&\frac{\partial N_{r\theta 1}}{\partial r}+\frac{1}{r}\frac{\partial N_{\theta\theta 1}}{\partial \theta}+\frac{2N_{r\theta 1}}{r}=0\\
&\frac{\partial M_{rr1}}{\partial r}+\frac{1}{r}\frac{\partial M_{r\theta 1}}{\partial \theta}+\frac{M_{rr1}-M_{\theta\theta 1}}{r}-Q_{rr1}=0\\
&\frac{\partial M_{r\theta 1}}{\partial r}+\frac{1}{r}\frac{\partial M_{\theta\theta 1}}{\partial \theta}+\frac{2M_{r\theta 1}}{r}-Q_{\theta\theta 1}=0\\
&\frac{\partial Q_{rr1}}{\partial r}+\frac{1}{r}\frac{\partial Q_{\theta\theta 1}}{\partial \theta}+\frac{Q_{rr1}}{r}+\frac{1}{r}\frac{\partial}{\partial r}\left(rN_{rr}^{0}\frac{\partial w_1}{\partial r}\right)\\
&+\frac{1}{r^2}\frac{\partial}{\partial \theta}\left(N_{\theta\theta}^{0}\frac{\partial w_1}{\partial \theta}\right)+\frac{2N_{r\theta}^{0}}{r}\frac{\partial^2 w_1}{\partial r\partial\theta}=0
\end{aligned} \tag{10}$$

where the force and moment resultants for the classical plate theory (CPT) can be expressed in term of infinitesimally small displacement as:

$$\begin{aligned}
N_{rr1}^{C}=&A_{11}\left(\frac{\partial u_1^{C}}{\partial r}\right)+A_{12}\left(\frac{u_1^{C}}{r}+\frac{1}{r}\frac{\partial v_1^{C}}{\partial\theta}\right)-B_{11}\left(\frac{\partial^2 w_1^{C}}{\partial r^2}\right)-\frac{T_N}{1-\nu}\\
&-B_{12}\left(\frac{1}{r}\frac{\partial w_1^{C}}{\partial r}+\frac{1}{r^2}\frac{\partial^2 w_1^{C}}{\partial\theta^2}\right)
\end{aligned} \tag{11a}$$

$$\begin{aligned}
N_{\theta\theta 1}^{C}=&A_{11}\left(\frac{u_1^{C}}{r}+\frac{1}{r}\frac{\partial v_1^{C}}{\partial\theta}\right)+A_{12}\left(\frac{\partial u_1^{C}}{\partial r}\right)-B_{11}\left(\frac{1}{r}\frac{\partial w_1^{C}}{\partial r}+\frac{1}{r^2}\frac{\partial^2 w_1^{C}}{\partial\theta^2}\right)\\
&-B_{12}\left(\frac{\partial^2 w_1^{C}}{\partial r^2}\right)-\frac{T_N}{1-\nu}
\end{aligned} \tag{11b}$$

$$N_{r\theta}^{C}=A_{33}\left(\frac{1}{r}\frac{\partial u_1^{C}}{\partial\theta}+\frac{\partial v_1^{C}}{\partial r}-\frac{v_1^{C}}{r}\right)-2B_{33}\left(\frac{1}{r}\frac{\partial^2 w_1^{C}}{\partial\theta\partial r}-\frac{1}{r^2}\frac{\partial w_1^{C}}{\partial\theta}\right) \tag{11c}$$

$$\begin{aligned}
M_{rr1}^{C}=&B_{11}\left(\frac{\partial u_1^{C}}{\partial r}\right)+B_{12}\left(\frac{u_1^{C}}{r}+\frac{1}{r}\frac{\partial v_1^{C}}{\partial\theta}\right)-D_{11}\left(\frac{\partial^2 w_1^{C}}{\partial r^2}\right)-\frac{T_M}{1-\nu}\\
&-D_{12}\left(\frac{1}{r}\frac{\partial w_1^{C}}{\partial r}+\frac{1}{r^2}\frac{\partial^2 w_1^{C}}{\partial\theta^2}\right)
\end{aligned} \tag{11d}$$

$$\begin{aligned}
M_{\theta\theta 1}^{C}=&B_{11}\left(\frac{u_1^{C}}{r}+\frac{1}{r}\frac{\partial v_1^{C}}{\partial\theta}\right)+B_{12}\left(\frac{\partial u_1^{C}}{\partial r}\right)-D_{11}\left(\frac{1}{r}\frac{\partial w_1^{C}}{\partial r}\right.\\
&\left.+\frac{1}{r^2}\frac{\partial^2 w_1^{C}}{\partial\theta^2}\right)-D_{12}\left(\frac{\partial^2 w_1^{C}}{\partial r^2}\right)-\frac{T_M}{1-\nu}
\end{aligned} \tag{11e}$$

$$M_{r\theta}^{C}=B_{33}\left(\frac{1}{r}\frac{\partial u_1^{C}}{\partial\theta}+\frac{\partial v_1^{C}}{\partial r}-\frac{v_1^{C}}{r}\right)-2D_{33}\left(\frac{1}{r}\frac{\partial^2 w_1^{C}}{\partial r\partial\theta}-\frac{1}{r^2}\frac{\partial w_1^{C}}{\partial\theta}\right) \tag{11f}$$

$$Q_{r1}^{C}=\frac{\partial M_{rr1}^{C}}{\partial r}+\frac{1}{r}\frac{\partial M_{r\theta 1}^{C}}{\partial\theta}+\frac{M_{rr1}^{C}-M_{\theta\theta 1}^{C}}{r} \tag{11g}$$

$$Q_{\theta 1}^{C}=\frac{\partial M_{r\theta 1}^{C}}{\partial r}+\frac{1}{r}\frac{\partial M_{\theta\theta 1}^{C}}{\partial\theta}+\frac{2M_{r\theta 1}^{C}}{r} \tag{11h}$$

Also, the plate stiffness coefficients are obtained from the following integrations:

$$\begin{aligned}
\left(A_{11},B_{11},D_{11}\right)&=\int_{-h/2}^{h/2}\frac{E(z)}{1-\nu^2}\left(1,z,z^2\right)\,dz\\
\left(A_{12},B_{12},D_{12}\right)&=\int_{-h/2}^{h/2}\frac{\nu E(z)}{1-\nu^2}\left(1,z,z^2\right)\,dz\\
\left(A_{33},B_{33},D_{33}\right)&=\int_{-h/2}^{h/2}\frac{E(z)}{2(1+\nu)}\left(1,z,z^2\right)dz
\end{aligned} \tag{12}$$

where the thermal terms T_N and T_M are defined as:

$$\begin{aligned}
T_N&=\int_{-h/2}^{h/2}E(z)\alpha(z)T(r,\theta,z)\,dz\\
T_M&=\int_{-h/2}^{h/2}E(z)\alpha(z)\,T(r,\theta,z)\,z\,dz
\end{aligned} \tag{13}$$

Also, these relations for the first order shear deformation plate theory (FSDT) can be written in the following form:

$$\begin{aligned}
N_{rr1}^{F}=&A_{11}\frac{\partial u_1^{F}}{\partial r}+A_{12}\left(\frac{u_1^{F}}{r}+\frac{1}{r}\frac{\partial v_1^{F}}{\partial\theta}\right)+B_{11}\frac{\partial\psi_{r1}}{\partial r}-\frac{T_N}{1-\nu}\\
&+B_{12}\left(\frac{\psi_{r1}}{r}+\frac{1}{r}\frac{\partial\psi_{\theta 1}}{\partial\theta}\right)
\end{aligned} \tag{14a}$$

$$\begin{aligned}
N_{\theta\theta 1}^{F}=&A_{11}\left(\frac{u_1^{F}}{r}+\frac{1}{r}\frac{\partial v_1^{F}}{\partial\theta}\right)+A_{12}\frac{\partial u_1^{F}}{\partial r}+B_{11}\left(\frac{\psi_{r1}}{r}+\frac{1}{r}\frac{\partial\psi_{\theta 1}}{\partial\theta}\right)+\\
&B_{12}\frac{\partial\psi_{r1}}{\partial r}-\frac{T_N}{1-\nu}
\end{aligned} \tag{14b}$$

$$N_{r\theta 1}^{F}=A_{33}\left(\frac{1}{r}\frac{\partial v_1^{F}}{\partial\theta}+\frac{\partial u_1^{F}}{\partial r}-\frac{u_1^{F}}{r}\right)+B_{33}\left(\frac{1}{r}\frac{\partial\psi_{r1}}{\partial\theta}+\frac{\partial\psi_{\theta 1}}{\partial r}-\frac{\psi_{\theta 1}}{r}\right) \tag{14c}$$

$$\begin{aligned}
M_{rr1}^{F}=&B_{11}\frac{\partial u_1^{F}}{\partial r}+B_{12}\left(\frac{u_1^{F}}{r}+\frac{1}{r}\frac{\partial v_1^{F}}{\partial\theta}\right)+D_{11}\frac{\partial\psi_{r1}}{\partial r}-\frac{T_M}{1-\nu}\\
&+D_{12}\left(\frac{\psi_{r1}}{r}+\frac{1}{r}\frac{\partial\psi_{\theta 1}}{\partial\theta}\right)
\end{aligned} \tag{14d}$$

$$\begin{aligned}
M_{\theta\theta 1}^{F}=&B_{11}\left(\frac{u_1^{F}}{r}+\frac{1}{r}\frac{\partial v_1^{F}}{\partial\theta}\right)+B_{12}\frac{\partial u_1^{F}}{\partial r}+D_{11}\left(\frac{\psi_{r1}}{r}+\frac{1}{r}\frac{\partial\psi_{\theta 1}}{\partial\theta}\right)\\
&+D_{12}\frac{\partial\psi_{r1}}{\partial r}-\frac{T_M}{1-\nu}
\end{aligned} \tag{14e}$$

$$M_{r\theta 1}^{F}=B_{33}\left(\frac{1}{r}\frac{\partial v_1^{F}}{\partial\theta}+\frac{\partial u_1^{F}}{\partial r}-\frac{u_1^{F}}{r}\right)+D_{33}\left(\frac{1}{r}\frac{\partial\psi_{r1}}{\partial\theta}+\frac{\partial\psi_{\theta 1}}{\partial r}-\frac{\psi_{\theta 1}}{r}\right) \tag{14f}$$

$$Q_{r1}^{F}=k^2A_{33}\left(\frac{\partial w_1^{F}}{\partial r}+\psi_{r1}\right) \tag{14g}$$

$$Q_{\theta 1}=k^2A_{33}\left(\frac{1}{r}\frac{\partial w_1^{F}}{\partial\theta}+\psi_{\theta 1}\right) \tag{14h}$$

Substituting the force and moment resultants from Equation (11) into Equation (10), the governing stability equations of FG annular plate based on CPT are obtained as:

$$\begin{aligned}
&A_{11}\left(\frac{\partial^2 u_1^{C}}{\partial r^2}+\frac{1}{r}\frac{\partial u_1^{C}}{\partial r}-\frac{u_1^{C}}{r^2}-\frac{1}{r^2}\frac{\partial v_1^{C}}{\partial\theta}+\frac{1}{r}\frac{\partial^2 v_1^{C}}{\partial r\partial\theta}\right)\\
&+A_{33}\left(\frac{1}{r^2}\frac{\partial^2 u_1}{\partial\theta^2}-\frac{1}{r}\frac{\partial v_1^{C}}{\partial r\partial\theta}-\frac{1}{r^2}\frac{\partial v_1^{C}}{\partial\theta}\right)-B_{11}\left(\frac{\partial^3 w_1^{C}}{\partial r^3}\right.\\
&\left.+\frac{1}{r}\frac{\partial^2 w_1^{C}}{\partial r^2}-\frac{1}{r^2}\frac{\partial w_1^{C}}{\partial r}-\frac{2}{r^3}\frac{\partial^2 w_1^{C}}{\partial\theta^2}+\frac{1}{r^2}\frac{\partial^3 w_1^{C}}{\partial r\partial\theta^2}\right)=0
\end{aligned} \tag{15a}$$

$$\begin{aligned}
&A_{11}\left(\frac{1}{r^2}\frac{\partial^2 v_1^{C}}{\partial\theta^2}+\frac{1}{r^2}\frac{\partial u_1^{C}}{\partial\theta}+\frac{1}{r}\frac{\partial^2 u_1^{C}}{\partial r\partial\theta}\right)+A_{33}\left(\frac{-1}{r}\frac{\partial^2 u_1^{C}}{\partial r\partial\theta}\right.\\
&\left.+\frac{1}{r^2}\frac{\partial u_1^{C}}{\partial\theta}+\frac{\partial^2 v_1^{C}}{\partial r^2}-\frac{v_1^{C}}{r^2}+\frac{1}{r}\frac{\partial v_1^{C}}{\partial r}\right)-B_{11}\left(\frac{1}{r^2}\frac{\partial^2 w_1^{C}}{\partial r\partial\theta}\right.\\
&\left.+\frac{1}{r^3}\frac{\partial^3 w_1^{C}}{\partial\theta^3}+\frac{1}{r}\frac{\partial^3 w_1^{C}}{\partial r^2\partial\theta}\right)=0
\end{aligned} \tag{15b}$$

$$B_{11}(\frac{\partial^3 u_1^C}{\partial r^3}+\frac{2}{r}\frac{\partial^2 u_1^C}{\partial r^2}-\frac{1}{r^2}\frac{\partial u_1^C}{\partial r}+\frac{u_1^C}{r^3}-\frac{1}{r^3}\frac{\partial v_1^C}{\partial \theta}-\frac{1}{r^2}\frac{\partial^2 v_1^C}{\partial r\partial\theta}+\frac{1}{r}\frac{\partial^3 v_1^C}{\partial r^2\partial\theta}+\frac{1}{r^2}\frac{\partial^3 u_1^C}{\partial\theta^2\partial r}-\frac{1}{r^3}\frac{\partial^2 u_1^C}{\partial\theta^2}-\frac{1}{r^3}\frac{\partial^3 v_1^C}{\partial\theta^3})-D_{11}(\frac{\partial^4 w_1^C}{\partial r^4}+\frac{2}{r}\frac{\partial^3 w_1^C}{\partial r^3}-\frac{1}{r^2}\frac{\partial^2 w_1^C}{\partial r^2}+\frac{1}{r^3}\frac{\partial w_1^C}{\partial r}-\frac{2}{r^2}\frac{\partial^4 w_1^C}{\partial r^2\partial\theta^2}-\frac{2}{r^3}\frac{\partial^3 w_1^C}{\partial\theta^2\partial r}+\frac{4}{r^4}\frac{\partial^2 w_1^C}{\partial\theta^2}+\frac{1}{r^4}\frac{\partial^4 w_1^C}{\partial\theta^4})+\frac{1}{r}\frac{\partial}{\partial r}(rN_{rr}^0\frac{\partial w_1^C}{\partial r})+\frac{1}{r^2}\frac{\partial}{\partial\theta}(N_{\theta\theta}^0\frac{\partial w_1^C}{\partial\theta})+\frac{2N_{r\theta}^0}{r}\frac{\partial^2 w_1^C}{\partial r\partial\theta}=0 \quad (15c)$$

Similarly, the stability equations of FG annular based on FSDT can be written in the following form:

$$A_{11}(\frac{\partial^2 u_1^F}{\partial r^2}+\frac{1}{r}\frac{\partial u_1^F}{\partial r}-\frac{u_1^F}{r^2}-\frac{1}{r^2}\frac{\partial v_1^F}{\partial\theta}+\frac{1}{r}\frac{\partial^2 v_1^F}{\partial r\partial\theta})+A_{33}(\frac{1}{r^2}\frac{\partial^2 u_1^F}{\partial\theta^2}-\frac{1}{r}\frac{\partial^2 v_1^F}{\partial r\partial\theta}-\frac{1}{r^2}\frac{\partial v_1^F}{\partial\theta})+B_{11}(\frac{\partial^2\psi_{r1}}{\partial r^2}+\frac{1}{r}\frac{\partial\psi_{r1}}{\partial r}-\frac{\psi_{r1}}{r^2}-\frac{1}{r^2}\frac{\partial\psi_{\theta1}}{\partial\theta}+\frac{1}{r}\frac{\partial^2\psi_{\theta1}}{\partial r\partial\theta})+B_{33}(\frac{1}{r^2}\frac{\partial^2\psi_r^1}{\partial\theta^2}-\frac{1}{r}\frac{\partial^2\psi_\theta^1}{\partial r\partial\theta}-\frac{1}{r^2}\frac{\partial\psi_\theta^1}{\partial\theta})=0 \quad (16a)$$

$$A_{11}(\frac{1}{r^2}\frac{\partial u_1^F}{\partial\theta}+\frac{1}{r}\frac{\partial^2 u_1^F}{\partial r\partial\theta}+\frac{1}{r^2}\frac{\partial^2 v_1^F}{\partial\theta^2})+A_{33}(\frac{-1}{r}\frac{\partial^2 u_1^F}{\partial r\partial\theta}+\frac{\partial^2 v_1^F}{\partial r^2}+\frac{1}{r^2}\frac{\partial u_1^F}{\partial\theta}+\frac{1}{r}\frac{\partial v_1^F}{\partial r}-\frac{v_1^F}{r^2})+B_{11}(\frac{1}{r}\frac{\partial\psi_{r1}}{\partial\theta}+\frac{1}{r^2}\frac{\partial^2\psi_{\theta1}}{\partial\theta^2}+\frac{1}{r}\frac{\partial^2\psi_{r1}}{\partial r\partial\theta})+B_{33}(\frac{-1}{r}\frac{\partial^2\psi_r^1}{\partial r\partial\theta}+\frac{\partial^2\psi_{\theta1}}{\partial r^2}+\frac{1}{r^2}\frac{\partial\psi_{\theta1}}{\partial\theta}+\frac{1}{r}\frac{\partial\psi_{\theta1}}{\partial r}-\frac{\psi_{\theta1}}{r^2})=0 \quad (16b)$$

$$B_{11}(\frac{\partial^2 u_1^F}{\partial r^2}+\frac{1}{r}\frac{\partial u_1^F}{\partial r}-\frac{u_1^F}{r^2}-\frac{1}{r^2}\frac{\partial v_1^F}{\partial\theta}+\frac{1}{r}\frac{\partial^2 v_1^F}{\partial r\partial\theta})+B_{33}(\frac{1}{r^2}\frac{\partial^2 u_1^F}{\partial\theta^2}-\frac{1}{r}\frac{\partial^2 v_1^F}{\partial r\partial\theta}-\frac{1}{r^2}\frac{\partial v_1^F}{\partial\theta})+D_{11}(\frac{\partial^2\psi_{r1}}{\partial r^2}+\frac{1}{r}\frac{\partial\psi_{r1}}{\partial r}-\frac{\psi_{r1}}{r^2}-\frac{1}{r^2}\frac{\partial\psi_{\theta1}}{\partial\theta}+\frac{1}{r}\frac{\partial^2\psi_{\theta1}}{\partial r\partial\theta})+D_{33}(\frac{1}{r^2}\frac{\partial^2\psi_r^1}{\partial\theta^2}-\frac{1}{r}\frac{\partial^2\psi_\theta^1}{\partial r\partial\theta}-\frac{1}{r^2}\frac{\partial\psi_\theta^1}{\partial\theta})-k^2A_{33}(\frac{\partial w_1^F}{\partial r}+\psi_{r1})=0 \quad (16c)$$

$$B_{11}(\frac{1}{r^2}\frac{\partial u_1^F}{\partial\theta}+\frac{1}{r}\frac{\partial^2 u_1^F}{\partial r\partial\theta}+\frac{1}{r^2}\frac{\partial^2 v_1^F}{\partial\theta^2})+B_{33}(\frac{-1}{r}\frac{\partial^2 u_1^F}{\partial r\partial\theta}+\frac{\partial^2 v_1^F}{\partial r^2}+\frac{1}{r^2}\frac{\partial u_1^F}{\partial\theta}+\frac{1}{r}\frac{\partial v_1^F}{\partial r}-\frac{v_1^F}{r^2})+D_{11}(\frac{1}{r}\frac{\partial\psi_{r1}}{\partial\theta}+\frac{1}{r^2}\frac{\partial^2\psi_{\theta1}}{\partial\theta^2}+\frac{1}{r}\frac{\partial^2\psi_{r1}}{\partial r\partial\theta})+D_{33}(\frac{-1}{r}\frac{\partial^2\psi^1_r}{\partial r\partial\theta}+\frac{\partial^2\psi_{\theta1}}{\partial r^2}+\frac{1}{r^2}\frac{\partial\psi_{\theta1}}{\partial\theta}+\frac{1}{r}\frac{\partial\psi_{\theta1}}{\partial r}-\frac{\psi_{\theta1}}{r^2})-k^2A_{33}(\frac{1}{r}\frac{\partial w_1^F}{\partial\theta}+\psi_{\theta1})=0 \quad (16d)$$

$$k^2A_{33}(\frac{\partial^2 w_1^F}{\partial r^2}+\frac{1}{r}\frac{\partial w_1^F}{\partial r}+\frac{1}{r^2}\frac{\partial^2 w_1^F}{\partial\theta^2}+\frac{\partial\psi_{r1}}{\partial r}+\frac{1}{r}\frac{\partial\psi_{\theta1}}{\partial\theta}+\frac{\psi_{r1}}{r})+\frac{1}{r}\frac{\partial}{\partial r}(rN_{rr}^0\frac{\partial w_1^F}{\partial r})+\frac{1}{r^2}\frac{\partial}{\partial\theta}(N_{\theta\theta}^0\frac{\partial w_1^F}{\partial\theta})+\frac{2N_{r\theta}^0}{r}\frac{\partial^2 w_1^F}{\partial r\partial\theta}=0 \quad (16e)$$

Both Equations (15) and (16) are two systems of highly coupled partial differential equations in terms of incremental in-plane and out of plane displacement components. Although these coupled equations can be solved using numerical methods, it may be difficult to solve them analytically in these forms. To find the analytical solutions for these two systems of equations, it is convenient to decouple them. Using the following method, either Equation (15) or Equation (16) will be decoupled.

4. A METHOD FOR DECOUPLING THE STABILITY EQUATIONS

Equation (15) can be changed to the following from:

$$A_{11}\frac{\partial\vartheta_1}{\partial r}+A_{33}\left(\frac{1}{r}\frac{\partial\vartheta_2}{\partial\theta}\right)-B_{11}\left(\frac{\partial}{\partial r}\left(\nabla^2 w_1^C\right)\right)=0 \quad (17a)$$

$$A_{11}\left(\frac{1}{r}\frac{\partial\vartheta_1}{\partial\theta}\right)-A_{33}\left(\frac{\partial\vartheta_2}{\partial r}\right)-B_{11}\left(\frac{1}{r}\frac{\partial}{\partial\theta}\left(\nabla^2 w_1^C\right)\right)=0 \quad (17b)$$

$$-B_{11}\nabla^2\vartheta_1+D_{11}\nabla^4 w_1^C+\frac{1}{r}\frac{\partial}{\partial r}\left(rN_{rr}^0\frac{\partial w_1^C}{\partial r}\right)+\frac{1}{r^2}\frac{\partial}{\partial\theta}\left(N_{\theta\theta}^0\frac{\partial w_1^C}{\partial\theta}\right)+\frac{2N_{r\theta}^0}{r}\frac{\partial^2 w_1^C}{\partial r\partial\theta}=0 \quad (17c)$$

where ∇^2 is two dimensional Laplace operator in the polar coordinates and $\nabla^4=\nabla^2\nabla^2$. Also, the variables ϑ_1 and ϑ_2 are defined as:

$$\vartheta_1=\frac{\partial u_1^C}{\partial r}+\frac{u_1^C}{r}+\frac{1}{r}\frac{\partial v_1^C}{\partial\theta}$$
$$\vartheta_2=\frac{1}{r}\frac{\partial u_1^C}{\partial\theta}-\frac{\partial v_1^C}{\partial r}-\frac{v_1^C}{r} \quad (18)$$

By differentiating Equations (17a) and (17b) with respect to r and θ, and performing some algebraic procedures, Equation (17) can be rewritten as:

$$\hat{D}\nabla^4 w_1^C+\frac{1}{r}\frac{\partial}{\partial r}\left(rN_{rr}^0\frac{\partial w_1^C}{\partial r}\right)+\frac{1}{r^2}\frac{\partial}{\partial\theta}\left(N_{\theta\theta}^0\frac{\partial w_1^C}{\partial\theta}\right)+\frac{2N_{r\theta}^0}{r}\frac{\partial^2 w_1^C}{\partial r\partial\theta}=0 \quad (19a)$$

$$\nabla^2\vartheta_2=0 \quad (19b)$$

where the parameter $\hat{D}$ is the equivalent flexural rigidity of FG plate which is written in the form of:

$$\hat{D}=\left(D_{11}-\frac{B_{11}^2}{A_{11}}\right) \tag{20}$$

Using Equations (17a) and (17b), the in-plane displacement are obtained in the form of:

$$\begin{aligned} u_1^C &= \frac{B_{11}}{A_{11}}\frac{dw_1^C}{dr} \\ v_1^C &= \frac{B_{11}}{A_{11}}\frac{1}{r}\frac{\partial w_1^C}{\partial \theta} \end{aligned} \tag{21}$$

Similarly, the stability Equation (16) based on the first order shear deformation plate theory can be simplified in the following equations:

$$A_{11}\frac{\partial \varphi_1^F}{\partial r}+A_{33}\frac{1}{r}\frac{\partial \varphi_2^F}{\partial \theta}+B_{11}\frac{\partial \varphi_3^F}{\partial r}+B_{33}\frac{1}{r}\frac{\partial \varphi_4^F}{\partial \theta}=0 \tag{22a}$$

$$A_{11}\frac{1}{r}\frac{\partial \varphi_1^F}{\partial \theta}-A_{33}\frac{\partial \varphi_2^F}{\partial r}+B_{11}\frac{1}{r}\frac{\partial \varphi_3^F}{\partial \theta}-B_{33}\frac{\partial \varphi_4^F}{\partial r}=0 \tag{22b}$$

$$\begin{aligned} &B_{11}\frac{\partial \varphi_1^F}{\partial r}+B_{33}\frac{1}{r}\frac{\partial \varphi_2^F}{\partial \theta}+D_{11}\frac{\partial \varphi_3^F}{\partial r}+D_{33}\frac{1}{r}\frac{\partial \varphi_4^F}{\partial \theta} \\ &-k^2A_{33}\left(\frac{\partial w_1^F}{\partial r}+\psi_{r1}\right)=0 \end{aligned} \tag{22c}$$

$$\begin{aligned} &A_{11}\frac{1}{r}\frac{\partial \varphi_1^F}{\partial \theta}-A_{33}\frac{\partial \varphi_2^F}{\partial r}+B_{11}\frac{1}{r}\frac{\partial \varphi_3^F}{\partial \theta}-B_{33}\frac{\partial \varphi_4^F}{\partial r} \\ &-k^2A_{33}\left(\frac{1}{r}\frac{\partial w_1^F}{\partial \theta}+\psi_{\theta 1}\right)=0 \end{aligned} \tag{22d}$$

$$\begin{aligned} &k^2A_{33}\left(\nabla^2 w_1^F+\varphi_2^F\right)+\frac{1}{r}\frac{\partial}{\partial r}\left(rN_{rr}^0\frac{\partial w_1^F}{\partial r}\right)+\frac{1}{r^2}\frac{\partial}{\partial \theta}\left(N_{\theta\theta}^0\frac{\partial w_1^F}{\partial \theta}\right) \\ &+\frac{2N_{r\theta}^0}{r}\frac{\partial^2 w_1^F}{\partial r\partial \theta}=0 \end{aligned} \tag{22e}$$

where the variables φ_1^F and φ_2^F are defined as:

$$\begin{aligned} \varphi_1^F &= \frac{\partial u_1^F}{\partial r}+\frac{u_1^F}{r}+\frac{1}{r}\frac{\partial v_1^F}{\partial \theta} \\ \varphi_2^F &= \frac{1}{r}\frac{\partial u_1^F}{\partial \theta}-\frac{\partial v_1^F}{\partial r}-\frac{v_1^F}{r} \\ \varphi_3^F &= \frac{\partial \psi_{r1}}{\partial r}+\frac{\psi_{r1}}{r}+\frac{1}{r}\frac{\partial \psi_{\theta 1}}{\partial \theta} \\ \varphi_4^F &= \frac{1}{r}\frac{\partial \psi_{r1}}{\partial \theta}-\frac{\partial \psi_{\theta 1}}{\partial r}-\frac{\psi_{\theta 1}}{r} \end{aligned} \tag{23}$$

Also, Equations (22a) and (22b) can be rewritten in the form:

$$\begin{aligned} B_{11}\frac{\partial \varphi_1^F}{\partial r}+B_{33}\frac{1}{r}\frac{\partial \varphi_2^F}{\partial \theta} &= -\frac{B_{11}^2}{A_{11}}\frac{\partial \varphi_3^F}{\partial r}-\frac{B_{33}B_{11}}{A_{11}}\frac{1}{r}\frac{\partial \varphi_4^F}{\partial \theta} \\ B_{11}\frac{1}{r}\frac{\partial \varphi_1^F}{\partial \theta}-B_{33}\frac{\partial \varphi_2^F}{\partial r} &= -\frac{B_{11}^2}{A_{11}}\frac{1}{r}\frac{\partial \varphi_3^F}{\partial \theta}+\frac{B_{33}B_{11}}{A_{11}}\frac{\partial \varphi_4^F}{\partial r} \end{aligned} \tag{24}$$

Substituting Equation (24) into Equations (22c) and (22d) yields:

$$\begin{aligned} &\left(D_{11}-\frac{B_{11}^2}{A_{11}}\right)\frac{\partial \varphi_3^F}{\partial r}+\left(D_{33}-\frac{B_{33}B_{11}}{A_{11}}\right)\left(\frac{1}{r}\frac{\partial \varphi_4^F}{\partial \theta}\right)- \\ &k^2A_{33}\left(\frac{\partial w_1^F}{\partial r}+\psi_{r1}\right)=0 \end{aligned} \tag{25a}$$

$$\begin{aligned} &\left(D_{11}-\frac{B_{11}^2}{A_{11}}\right)\left(\frac{1}{r}\frac{\partial \varphi_3^F}{\partial \theta}\right)+\left(D_{33}-\frac{B_{33}B_{11}}{A_{11}}\right)\frac{\partial \varphi_4^F}{\partial r} \\ &-k^2A_{33}\left(\frac{1}{r}\frac{\partial w_1^F}{\partial \theta}+\psi_{\theta 1}\right)=0 \end{aligned} \tag{25b}$$

Differentiation of Equations (25a) and (25b) with respect to r and θ together with Equation (22e), and doing some algebraic operations the following decoupled partial differential equations are obtained:

$$\begin{aligned} &\hat{D}\nabla^4 w_1^F+\frac{1}{r}\frac{\partial}{\partial r}(rN_{rr}^0\frac{\partial w_1^F}{\partial r})+\frac{1}{r^2}\frac{\partial}{\partial \theta}(N_{\theta\theta}^0\frac{\partial w_1^F}{\partial \theta}) \\ &+\frac{2N_{r\theta}^0}{r}\frac{\partial^2 w_1^F}{\partial r\partial \theta}=-\frac{\hat{D}}{k^2A_{33}}\nabla^2(\frac{1}{r}\frac{\partial}{\partial r}(rN_{rr}^0\frac{\partial w_1^F}{\partial r}) \\ &+\frac{1}{r^2}\frac{\partial}{\partial \theta}(N_{\theta\theta}^0\frac{\partial w_1^F}{\partial \theta})+\frac{2N_{r\theta}^0}{r}\frac{\partial^2 w_1^F}{\partial r\partial \theta}) \end{aligned} \tag{26a}$$

$$\hat{C}\nabla^2\varphi_4^F-k^2A_{33}\varphi_4^F=0 \tag{26b}$$

where the variable $\hat{C}$ denotes the equivalent flexural rigidity of FG plate defined as:

$$\hat{C}=D_{33}-\frac{B_{11}B_{33}}{A_{11}} \tag{27}$$

By considering Equations (25a) and (25b) and doing some algebraic procedures, it is easy to show that:

$$\begin{aligned} \psi_{r1} &= -\frac{\partial}{\partial r}(w_1^F+\frac{\hat{D}}{k^2A_{33}}\nabla^2 w_1^F+\frac{\hat{D}}{k^4A_{33}^2}(\frac{1}{r}\frac{\partial}{\partial r}(rN_{rr}^0\frac{\partial w_1^F}{\partial r}) \\ &+\frac{1}{r^2}\frac{\partial}{\partial \theta}(N_{\theta\theta}^0\frac{\partial w_1^F}{\partial \theta})+\frac{2N_{r\theta}^0}{r}\frac{\partial^2 w_1^F}{\partial r\partial \theta}))+\frac{\hat{C}}{k^2A_{33}}(\frac{1}{r}\frac{\partial \varphi_4^F}{\partial \theta}) \\ \psi_{\theta 1} &= -\frac{1}{r}\frac{\partial}{\partial \theta}(w_1^F+\frac{\hat{D}}{k^2A_{33}}\nabla^2 w_1^F+\frac{\hat{D}}{k^4A_{33}^2}(\frac{1}{r}\frac{\partial}{\partial r}(rN_{rr}^0\frac{\partial w_1^F}{\partial r}) \\ &+\frac{1}{r^2}\frac{\partial}{\partial \theta}(N_{\theta\theta}^0\frac{\partial w_1^F}{\partial \theta})+\frac{2N_{r\theta}^0}{r}\frac{\partial^2 w_1^F}{\partial r\partial \theta}))-\frac{\hat{C}}{k^2A_{33}}(\frac{\partial \varphi_4^F}{\partial r}) \end{aligned} \tag{28}$$

Performing some algebraic operations on Equation (24), the in-plane displacement can be obtained as:

$$u_1^F=-\frac{B_{11}}{A_{11}}\psi_{r1} \tag{29a}$$

$$v_1^F=-\frac{B_{11}}{A_{11}}\psi_{\theta 1} \tag{29b}$$

Therefore, both the classical and first order shear deformation stability equations of the FG plate have been decoupled to the Equations (19) and (26), respectively. In order to buckling analysis of FG annular plates subjected to mechanical and/or thermal load, these equations should be solved.

5. BUCKLING ANALYSIS UNDER MECHANICAL AND THERMAL LOADS

Consider a FG annular circular plate subjected to uniform in-plane force P_e and uniform temperature T with arbitrary boundary conditions on inner and outer

circular edges. To obtain the critical buckling load and/or temperature, the distribution of the in-plane forces should be determined in the pre-buckling configuration. Solving the membrane form of the equilibrium equations, the pre-buckling forces are obtained as:

$$\begin{aligned} N_{rr}^{0} &= -P_e \\ N_{\theta\theta}^{0} &= -P_e \\ N_{r\theta}^{0} &= 0 \end{aligned} \tag{30}$$

where,

$$P_e = \begin{cases} P & \text{for mechanical buckling analysis} \\ \dfrac{T_N}{1-\nu} & \text{for therma l buckling analysis} \end{cases} \tag{31}$$

By substituting Equation (30) into Equations (19), the CPT stability equation is rewritten in the following form

$$\hat{D}\nabla^4 w_1^C - P_e\nabla^2 w_1^C = 0 \tag{32}$$

Also, by substituting Equation (30) into Equation (26), the FSDT stability equations are obtained as:

$$\begin{aligned} &\hat{D}\left(1-\frac{P_e}{k^2 A_{33}}\right)\nabla^4 w_1^F - P_e\nabla^2 w_1^F = 0 \\ &\hat{C}\nabla^2\varphi_4 - k^2 A_{33}\varphi_4 = 0 \end{aligned} \tag{33}$$

6. SOLUTION

In order to take into account both the symmetric and asymmetric buckling modes of the FG plate under mechanical and thermal loads, let us consider the following forms for the transverse displacement, w_1, and the function φ_4^F [27]:

$$\begin{aligned} w_1 &= \sum_{m=0}^{\infty} w_m(r)\cos(m\theta) \\ \varphi_4^F &= \sum_{m=0}^{\infty} \varphi_m(r)\sin(m\theta) \end{aligned} \tag{34}$$

Upon substituting the above series into the decoupled Equations (32) and (33), three ordinary differential equations are obtained. The solutions of these differential equations for symmetric solutions ($m=0$) are obtained as:

$$w_1^C = C_1 + C_2\ln(r) + C_3 J_0\left(\sqrt{\frac{P_e}{\hat{D}}}r\right) + C_4 Y_0\left(\sqrt{\frac{P_e}{\hat{D}}}r\right) \tag{35a}$$

$$\begin{aligned} w_1^F = {} & C_1 + C_2\ln(r) + C_3 J_0\left(k\sqrt{\frac{P_e A_{33}}{\hat{D}(k^2 A_{33} - P_e)}}r\right) \\ & + C_4 Y_0\left(k\sqrt{\frac{P_e A_{33}}{\hat{D}(k^2 A_{33} - P_e)}}r\right) \end{aligned} \tag{35b}$$

$$\varphi_m^F(r) = C_5 I_0\left(k\sqrt{\frac{A_{33}}{C}}r\right) + C_6 K_0\left(k\sqrt{\frac{A_{33}}{C}}r\right) \tag{35c}$$

where J and Y are the first and second kind of ordinary Bessel functions, respectively. Also, for asymmetric solutions ($m\geq 1$) the solutions for CPT and FSDT equations are obtained as:

$$w_1^C = C_1 r^m + C_2 r^{-m} + C_3 J_m\left(\sqrt{\frac{P_e}{\hat{D}}}r\right) + C_4 Y_m\left(\sqrt{\frac{P_e}{\hat{D}}}r\right) \tag{36a}$$

$$\begin{aligned} w_1^F = {} & C_1 r^m + C_2 r^{-m} + C_3 J_m\left(k\sqrt{\frac{P_e A_{33}}{\hat{D}(k^2 A_{33} - P_e)}}r\right) \\ & + C_4 Y_m\left(k\sqrt{\frac{P_e A_{33}}{\hat{D}(k^2 A_{33} - P_e)}}r\right) \end{aligned} \tag{36b}$$

$$\varphi_m^F(r) = C_5 I_m\left(k\sqrt{\frac{A_{33}}{C}}r\right) + C_6 K_m\left(k\sqrt{\frac{A_{33}}{C}}r\right) \tag{36c}$$

where I and K are the first and second kind of the modified Bessel functions. Imposing the boundary conditions at the circular edges of the plate leads to a set of four or six homogenous algebraic equations for $m=0$ or $m\geq 1$, respectively in FSDT and four equations in CPT. Setting the determinant of the constant coefficients equal to zero, the critical buckling load and/or temperature can be obtained.

7. BOUNDARY CONDITIONS

Here, three classic boundary conditions are considered on the circular edges containing simply supported, clamped and free edge.

For the simply supported boundary condition it can be written as:

$$\text{CPT: } w_1^C = M_{rr}^C = 0 \text{ at } r = a, b \tag{37a}$$

$$\text{FSDT: } w_1^F = M_{rr}^F = 0 \text{ at } r = a, b \tag{37b}$$

For the clamped boundary condition it is easy to show that:

$$\text{CPT: } w_1^C = \frac{dw_1^C}{dr} = 0 \text{ at } r = a, b \tag{38a}$$

$$\text{FSDT: } w_1^F = \psi_{r1} = 0 \text{ at } r = a, b \tag{38b}$$

Finally, the free boundary condition requires:

$$\text{CPT: } M_{r\theta}^C = Q_r^C = 0 \text{ at } r = a, b \tag{39a}$$

$$\text{FSDT: } M_{rr}^F = M_{r\theta}^F = Q_{rr}^F + N_{rr0}\frac{\partial w_1^F}{\partial r} = 0 \text{ at } r = a, b \tag{39b}$$

The eight possible boundary conditions containing SS, CC, CS, SC, CF, FC, CS and SF have been considered. It is noticeable that, for example, CS denotes an annular plate with clamped inner and simply supported outer radii.

8. NUMERICAL RESULTS AND DISCUSSION

For numerical calculations, it is assumed that the functionally graded plate is composed of aluminum with $E_m = 70GPa$ and alumina with $E_c = 380GPa$. The Poisson ratio of the plate is assumed to be constant through the thickness and equal to 0.3. Here, the non-dimensional buckling load is defined as:

$$P_{cr} = \frac{Nb^2}{D_c} \tag{40}$$

where

$$D_c = \frac{E_c h^3}{12\,(1-\nu^2)} \tag{41}$$

In order to verify the accuracy of the present analysis, the numerical results are compared with the available results for mechanical and thermal buckling load of annular and circular plates based on CPT and FSDT in Refs. [5] and [16], respectively. The results presented in Ref. [5] have been obtained for the homogenous annular plates and those reported in Ref. [16] have been presented for FG circular plates.

Table 1 shows a comparison between the critical buckling load of a FG annular plate with $n = 0$ and those presented in Ref. [5] for the homogenous plates based on the classical plate theory.

Table 2 shows the comparison of the critical buckling temperature of FG annular plate by assuming that the inner radius, a, is very small (e.g. $a = 10^{-12}(m)$) based on FSDT with those obtained for the FG simply supported solid circular plates. It can be seen from Tables 1 and 2 that the results are in good agreement with those reported in the literature.

TABLE 1. Comparison of the results ($\sqrt{P_{cr}}$) with Ref. [5] based on the classical plate theory ($n = 0$)

B. C.		$a/b = 0$	$a/b = 0.1$	$a/b = 0.3$	$a/b = 0.5$	$a/b = 0.7$	$a/b = 0.9$
CC	Ref. [5]	5.135(1)	6.68 (2)	8.63(2)	12.15(4)	20.27(7)	60.89(24)
	Present	5.135(1)	6.710(1)	8.636(2)	12.155(4)	20.282(7)	60.890(23)
SC	Ref. [5]	5.135(1)	6.02(1)	7.06(0)	9.42(0)	15.31(0)	45.20(0)
	Present	5.135(1)	5.990(1)	7.058(0)	9.416(0)	15.304(0)	45.199(0)
FC	Ref. [5]	3.832(0)	3.62(0)	3.19(0)	3.65(0)	5.52(0)	15.89(0)
	Present	3.832(0)	3.626(0)	3.187(0)	3.645(0)	5.523(0)	15.875(0)
CS	Ref. [5]	3.625(1)	4.71(1)	6.16(0)	8.73(0)	14.73(0)	44.69(0)
	Present	3.624(0)	4.690(1)	6.155(0)	8.726(0)	17.724(0)	44.688(0)
SS	Ref. [5]	3.625(1)	4.20(1)	4.75(0)	6.40(0)	10.52(0)	31.43(0)
	Present	3.624(0)	4.205(0)	4.749(0)	6.400(0)	10.523(0)	31.429(0)
FS	Ref. [5]	2.049(0)	1.98(0)	1.61(0)	1.32(0)	1.14(0)	1.01(0)
	Present	2.049(0)	1.976(0)	1.612(0)	1.323(0)	1.135(0)	1.005(0)
CF	Ref. [5]	0.0(1)	1.49(1)	2.18(2)	3.14(1)	5.19(0)	15.61(0)
	Present	0.0(1)	1.490(1)	2.167(2)	3.143(1)	5.194(0)	15.605(0)
SF	Ref. [5]	0.0(1)	1.12(1)	1.34(1)	1.32(0)	1.14(0)	1.01(0)
	Present	0.0(1)	1.124(1)	1.341(1)	1.323(0)	1.135(0)	1.005(0)

TABLE 2. Comparison of the critical buckling temperature SS annular plates with those obtained in Ref. [16] for circular plates based on FSDT.

n		$h/a = 0.05$	$h/a = 0.08$	$h/a = 0.1$
0	Ref. [16]	90.956	232.848	363.825
	Present	90.955	232.904	363.147
1	Ref. [16]	42.255	108.174	169.023
	Present	42.262	108.224	169.026
5	Ref. [16]	38.648	98.941	154.595
	Present	38.632	98.847	154.388
10	Ref. [16]	39.731	101.713	158.927
	Present	39.699	101.514	158.330

TABLE 3. The effect of annularity on the non-dimensional buckling load, P_{cr}, and critical buckling temperature, $T_{cr}(^{\circ}C)$ and ($h/b=0.02$, $n=1$).

	a/b		CC	SS	CS	SC	CF	FC	FS	SF
P_{cr}	0.2	CPT	28.055(2)	9.389(0)	14.299(1)	20.636(1)	1.687(1)	5.436(0)	1.617(0)	0.783 (1)
		FSDT	27.831(2)	9.369(0)	14.239(1)	20.548(1)	1.682(1)	5.430(0)	1.617(0)	0.782(1)
	0.4	CPT	50.840(3)	14.587(0)	26.024(0)	31.909(0)	3.346(2)	5.427(0)	1.051(0)	0.981(1)
		FSDT	50.204(3)	14.544(0)	25.867(0)	31.710(0)	3.324(2)	5.421(0)	1.050(0)	0.980(1)
	0.6	CPT	115.164(5)	31.369(0)	60.050(0)	67.117(0)	7.673(0)	9.240(0)	0.741(0)	0.741(0)
		FSDT	112.087(5)	31.178(0)	59.256(0)	66.216(0)	7.662(0)	9.224(0)	0.741(0)	0.741(0)
	0.8	CPT	4613797(11)	123.454(0)	246.036(0)	258.189(0)	30.166(0)	32.488(0)	0.565(0)	0.565(0)
		FSDT	417.044(11)	120.575(0)	233.579(0)	245.043(0)	29.991(0)	32.286(0)	0.564(0)	0.564(0)
T_{cr}	0.2	CPT	90.607(2)	30.260(0)	46.180(1)	66.647(1)	5.448(1)	17.557(0)	5.224(0)	2.531(1)
		FSDT	89.884(2)	30.260(0)	45.986(1)	66.363(1)	5.433(1)	17.538(0)	5.222(0)	2.528(1)
	0.4	CPT	164.193(3)	47.109(0)	84.047(0)	103.055(0)	10.807(2)	17.528(0)	3.394(0)	3.171(1)
		FSDT	162.137(3)	46.971(0)	83.539(0)	102.412(0)	10.737(2)	17.510(0)	3.393(0)	3.165(1)
	0.6	CPT	371.931(5)	101.309(0)	193.937(0)	216.760(0)	24.783(0)	29.843(0)	2.394(0)	2.394(0)
		FSDT	361.994(5)	100.692(0)	191.372(0)	213.850(0)	24.746(0)	29.790(0)	2.394(0)	2.394(0)
	0.8	CPT	1491.405(11)	398.702(0)	794.591(0)	833.838(0)	97.423(0)	104.924(0)	1.824(0)	1.824 (0)
		FSDT	1346.872(11)	389.404(0)	754.361(0)	791.382(0)	96.859(0)	104.270(0)	1.824(0)	1.824(0)

TABLE 4. The effect of thickness radius ratio on the non-dimensional buckling load, P_{cr}, and critical buckling temperature, $T_{cr}(^{\circ}C)$, for ($a/b=0.5$, $n=1$).

	h/b		CC	SS	CS	SC	CF	FC	FS	SF
P_{cr}	0.02	CPT	73.645(4)	20.422(0)	37.953(0)	44.192(0)	4.926(1)	6.624(0)	0.872(0)	0.872(0)
		FSDT	72.339(4)	20.340(0)	37.627(0)	43.806(0)	4.913(1)	6.616(0)	0.872(0)	0.872(0)
	0.05	CPT	73.645(4)	20.422(0)	37.953(0)	44.192(0)	4.926(1)	6.624(0)	0.872(0)	0.872(0)
		FSDT	66.289(4)	19.920(0)	36.008(0)	41.881(0)	4.870(1)	6.572(0)	0.871(0)	0.872(0)
	0.1	CPT	73.645(4)	20.422(0)	37.953(0)	44.192(0)	4.926(1)	6.624(0)	0.872(0)	0.872(0)
		FSDT	51.474 (4)	18.553(0)	31.210(0)	36.204(0)	4.745(1)	6.419(0)	0.869(0)	0.869(0)
T_{cr}	0.02	CPT	237.842(4)	65.954(0)	122.572(0)	142.723(0)	15.909(1)	21.394(0)	2.818(0)	2.818(0)
		FSDT	233.624(4)	65.689(0)	121.521(0)	141.474(0)	15.867(1)	21.367(0)	2.818(0)	2.818(0)
	0.05	CPT	1486.515(4)	412.213(0)	766.077(0)	892.023(0)	99.435(1)	133.718(0)	17.616(0)	17.616(0)
		FSDT	1338.041(4)	402.090(0)	726.812(0)	845.373(0)	98.310(1)	132.657(0)	17.598(0)	17.598(0)
	0.1	CPT	5946.062(4)	1648.855(0)	3064.308(0)	3568.094(0)	397.742(1)	534.872(0)	70.466(0)	70.466(0)
		FSDT	4156.006(4)	1498.008(0)	2519.933(0)	2923.120(0)	383.096(1)	518.303(0)	70.170(0)	70.170(0)

Table 3, presents the critical buckling load and temperature together with the mode number for the FG annular plates with eight possible combination of the boundary conditions versus the aspect ratio a/b. In this table, the numbers in bracket show the mode number. However, when $m=0$, it means that the buckling mode is symmetric. From this table, it can be seen that for some boundary conditions as the annularity varies, the mode number may be changed. Also, this table shows that the critical buckling load and temperature increases as the annularity increases expect for the plate with FS and SF boundary conditions. Also, in SF and FS boundary conditions for $a/b>0.6$, the critical buckling load and temperature are the same.

Table 4 shows the critical buckling load and temperature versus the variation of thickness-radius ratio, h/b for $b/a=2$ and $n=1$ for a FG plate with eight possible boundary conditions. It can be seen that

using FSDT, by increasing the thickness-radius ratio, the non dimensional critical buckling load decreases. It is noticeable that since the critical load is a non-dimensional parameter with respect to b/h, it is neutral with respect to variation of thickness-radius ratio in the classical plate theory. The significant note which can be found from this table is that the variation of thickness-radius ratio does not change the buckling mode number. Also, for SF and FS boundary conditions the critical buckling load and temperature are similar. Table 5 presents the critical buckling load and temperature for a FG plate with CC boundary conditions versus the variation of h/b and n. It can be seen from this table that the mode number may vary with the variation of power law index and radius-thickness ratio. Also, Table 5 shows that when $b/h \geq 20$, buckling occurs in a same mode number based on two theories. By comparing the results of two theories, it can be seen that as the radius-thickness ratio increases, the difference between the results increases. In fact, by increasing the plate thickness, the accuracy of the classical plate theory decreases.

Figures 2 to 6 show the effects of annularity on the stability of FG annular plates versus the power law index, annularity and radius-thickness ratio for various boundary conditions. In these figures, the ratio $a/b = 0$ denotes the solid circular plate and $a/b \cong 1$ denotes a thin ring.

Figures 2 and 3 show the non-dimensional critical buckling load for different boundary conditions versus the variation of annularity. These figures show that for SS, SC, CS, CC and CF plates as the plate annularity increases, the critical buckling load increases because the plate stiffness increases. Also, from this figure it is observed that for a plate with FS boundary condition by increasing the plate annularity the critical buckling load decreases since by increasing the annularity stiffness of this plate decreases. For FC boundary condition the critical buckling load decreases first and then increases but for SF boundary condition the critical buckling load first increases and then decreases.

Figure 4 shows the effect of power law index n, on the non-dimensional critical buckling load. From this figure, it can be seen that as the power law index increases, the critical buckling load decreases and this decrease is rapid for large amounts of the annularity. It is clear that when $n = 0$ (plate is fully ceramic,) the critical buckling load is maximum. Therefore, when the highest critical buckling load is required, the ceramic isotropic plates are suitable.

TABLE 5. The effect of n and b/h on the non-dimensional buckling load, P_{cr}, and critical buckling temperature, $T_{cr}(^{\circ}C)$, for the plate with CC boundary condition and $b/a = 3$.

	n		$b/h=100$	$b/h=50$	$b/h=20$	$b/h=10$	$b/h=5$
P_{cr}	0	CPT	82.799 (2)	82.799(2)	82.799(2)	82.799(2)	82.799(2)
		FSDT	82.555 (2)	81.835(2)	77.186 (2)	64.032 (3)	39.343(3)
	0.5	CPT	53.674(2)	53.674 (2)	53.674(2)	53.674(2)	53.674(2)
		FSDT	53.533(2)	53.116(2)	50.406(2)	42.543 (3)	26.976(3)
	1	CPT	41.270(2)	41.270(2)	41.270(2)	41.270(2)	41.270(2)
		FSDT	41.168(2)	40.865(2)	38.886(2)	33.078(3)	21.290(3)
	2	CPT	32.204(2)	32.204(2)	32.204(2)	32.204(2)	32.204(2)
		FSDT	32.123(2)	31.883(2)	30.321(2)	25.747(3)	16.515(3)
	5	CPT	27.234(2)	27.234(2)	27.234(2)	27.234(2)	27.234(2)
		FSDT	27.151(2)	26.908(2)	25.341(2)	20.935(3)	12.767(3)
T_{cr}	0	CPT	71.725(2)	286.901(2)	1793.134(2)	7172.537(2)	28690.149(2)
		FSDT	71.513(2)	283.560(2)	1671.576(2)	5546.823(3)	13632.376(3)
	0.5	CPT	40.637(2)	162.551(2)	1015.942(2)	4063.769(2)	16255.077(2)
		FSDT	40.531(2)	160.862(2)	954.093(2)	3221.011(3)	8169.818(3)
	1	PTC	33.321(2)	133.286(2)	833.040(2)	3332.163(2)	13328.651(2)
		FSDT	33.238(2)	131.976(2)	784.906(2)	2670.753(3)	6875.786(3)
	2	CPT	29.541(2)	118.165(2)	738.537(2)	2954.149(2)	11816.598(2)
		FSDT	29.467(2)	116.989(2)	695.349(2)	2361.833(3)	6059.909(3)
	5	CPT	30.477(2)	121.909(2)	761.935(2)	3047.738(2)	12190.955(2)
		FSDT	30.385(2)	120.451(2)	708.984(2)	2342.816(3)	5715.268(3)

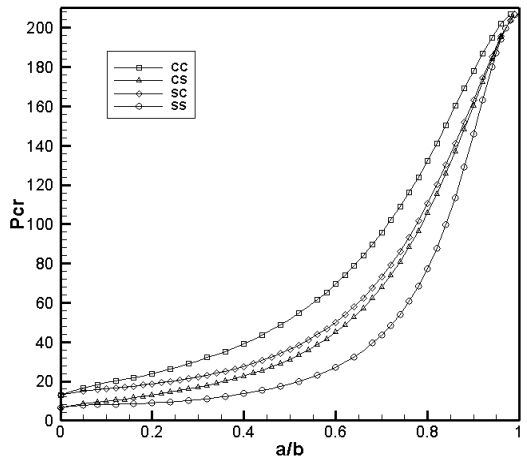

Figure 2. The critical buckling load of FG annular plate versus the annularity based on FSDT ($n = 1, b/h = 10$)

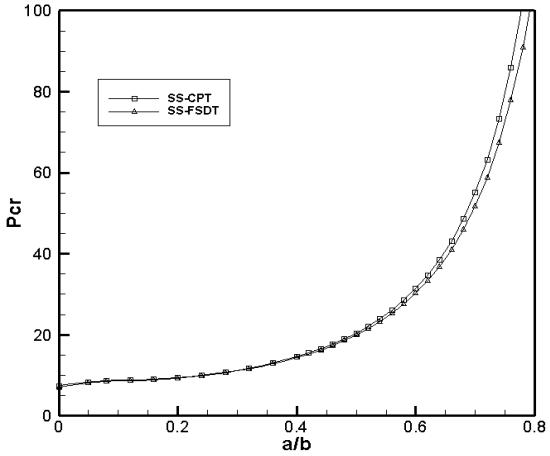

Figure 5. Comparison of the critical buckling load of simply supported FG annular based on the CPT and FSDT ($n=1, b/h=20$)

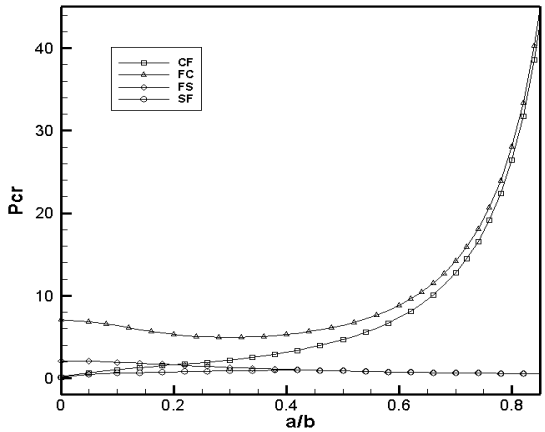

Figure 3. The critical buckling load of FG annular plate having free boundary condition versus the annularity based on FSDT ($n=1, b/h=10$)

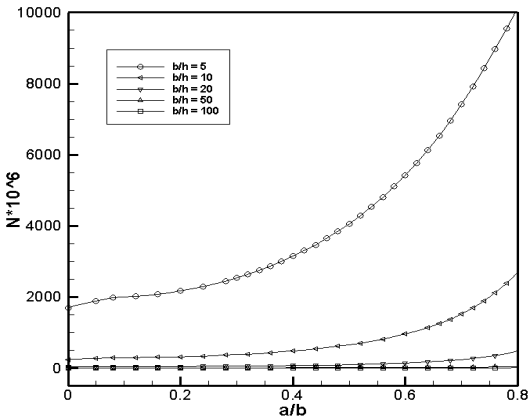

Figure 6. The effect of annularity and radius-thickness ratio on the critical buckling load of a simply supported FG annular plate based on FSDT ($n = 1$)

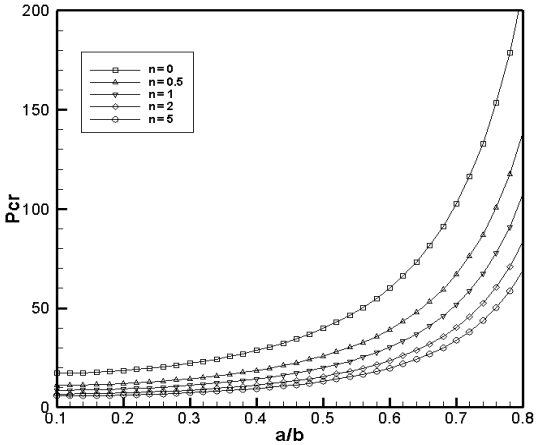

Figure 4. The critical buckling load of simply supported FG annular plate based on FSDT ($b/h = 20$)

Figure 5 shows a comparison between two theories. It shows that as the annularity of the plate increases, the difference between the classical and first order shear deformation plate theories increases because the flexural rigidity of the plate becomes larger.

The variation of critical buckling load and temperature with respect to annularity is presented for different values of the radius-thickness ratio in Figures 6 and 7, respectively. These figures show that by increasing the plate thickness, the critical buckling load and temperature increases. Also, it can be seen that as the parameter a/b increases, the thickness of the plate has more effect on the critical buckling load and temperature. Therefore, for the plates with small annularity, the thickness of the plate has negligible effect on the critical buckling load and temperature.

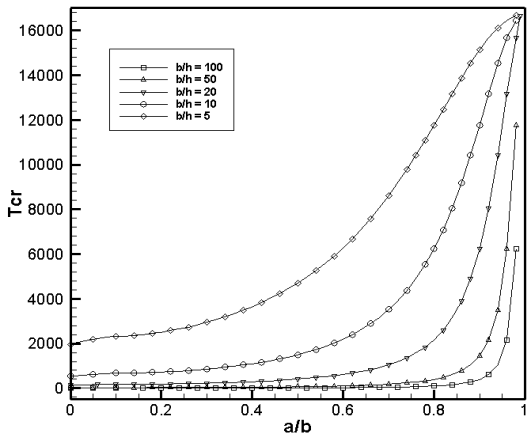

Figure 7. Critical buckling temperature of FG annular plate under various annularity a/b and b/h ($n=1$) for SS boundary condition

In Figure 8, the mode shape plots for a FG annular plate with eight possible boundary conditions are presented. It can be seen that the buckling mode number is different for different boundary conditions. For example, for CC boundary condition the mode number is $m=4$, for CF, $m=2$, for SF, $m=1$ and for the other boundary conditions the buckling occurs in symmetric mode (i.e. $m=0$).

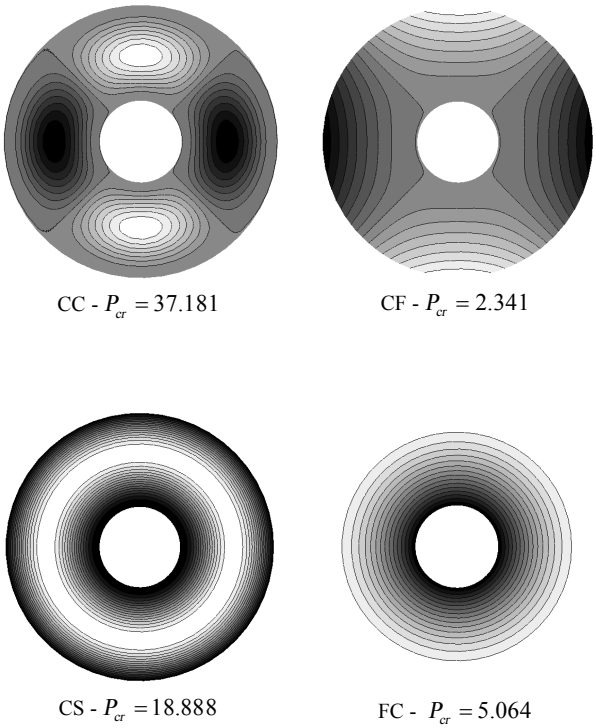

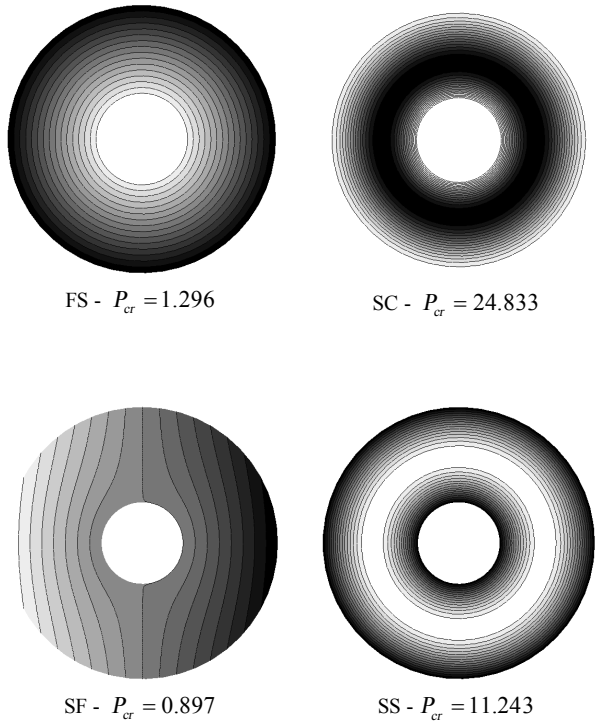

Figure 8. Mode shape plots of the FG annular plate with various boundary conditions ($n=1, b/h=20, a/b=0.3$).

9. CONCLUSIONS

In the present article, symmetric and asymmetric buckling modes of functionally graded thin and moderately thick annular plates have been studied. The equilibrium and stability equations have been obtained based on both the classical and first order shear deformation plate theories for the annular plate subjected to in-plane loads acting on the physical neutral surface. Using some functions and carrying out some algebraic manipulations, the highly coupled stability differential equations of the FG annular plates have been decoupled and the analytical solution has been presented for these decoupled equations. The critical buckling loads and mode shape plots have been presented for FG annular plates with eight possible boundary conditions. The following conclusions have been obtained:

I. As the plate annularity increases, the critical buckling load and/or temperature increase expect for the plate with FC, FS and SF boundary conditions.
II. The mode number may vary with the variation of power law index, annularity and radius-thickness ratio.
III. By increasing the power law index, the critical buckling load and/or temperature decreases.

7. REFERENCES

1. Koizumi, M., "Fgm activities in japan", ***Composites Part B: Engineering***, Vol. 28, No. 1, (1997), 1-4.
2. Byrd, L. W. and Birman, V., "Modeling and analysis of functionally graded materials and structures", ***Applied Mechanics Reviews***, Vol. 60, (2007), 195-216.
3. Suresh, S., Mortensen, A. and Suresh, S., "Fundamentals of functionally graded materials", IOM Communications Limited London, United Kingdom, (1998).
4. Dean, W., "The elastic stability of an annular plate", ***Proceedings of the Royal Society of London. Series A***, Vol. 106, No. 737, (1924), 268-284.
5. Yamaki, N., "Buckling of a thin annular plate under uniform compression", ***Journal of Applied Mechanics, Transaction of ASME***, Vol. 25, (1958), 267-273.
6. Elishakoff, I. and Stavsky, Y., "Axisymmetric buckling of certain annular composite plates", ***International Journal of Solids and Structures***, Vol. 11, No. 12, (1975), 1347-1356.
7. Srinivasan, R. and Ramachandra, L., "Axisymmetric buckling and post-buckling of bimodulus annular plates", ***Engineering Structures***, Vol. 11, No. 3, (1989), 195-198.
8. Chang, J.-S., "Axisymmetric buckling of moderately thick polar orthotropic annular plates", ***Composites Science and Technology***, Vol. 52, No. 1, (1994), 73-83.
9. Ciancio, P. and Reyes, J., "Buckling of circular, annular plates of continuously variable thickness used as internal bulkheads in submersibles", ***Ocean Engineering***, Vol. 30, No. 11, (2003), 1323-1333.
10. Xu, R., Wang, Y. and Chen, W., "Axisymmetric buckling of transversely isotropic circular and annular plates", ***Archive of Applied Mechanics***, Vol. 74, No. 10, (2005), 692-703.
11. Arafat, H. N., Faris, W. and Nayfeh, A. H., "Vibrations and buckling of annular and circular plates subjected to a thermal load", in 44 th AIAA/ASME/ASCE/AHS/ASC Structures, Structural Dynamics, and Materials Conference, (2003).
12. Ma, L. and Wang, T., "Relationships between axisymmetric bending and buckling solutions of fgm circular plates based on third-order plate theory and classical plate theory", ***International Journal of Solids and Structures***, Vol. 41, No. 1, (2004), 85-101.
13. Birman, V. and Simitses, G. J., "Buckling and bending of cylindrically orthotropic annular plates", ***Composites Engineering***, Vol. 1, No. 1, (1991), 41-47.
14. Najafizadeh, M. and Eslami, M., "Buckling analysis of circular plates of functionally graded materials under uniform radial compression", ***International Journal of Mechanical Sciences***, Vol. 44, No. 12, (2002), 2479-2493.
15. Najafizadeh, M. and Eslami, M., "Thermoelastic stability of orthotropic circular plates", ***Journal of Thermal Stresses***, Vol. 25, No. 10, (2002), 985-1005.
16. Najafizadeh, M. and Eslami, M., "First-order-theory-based thermoelastic stability of functionally graded material circular plates", ***AIAA Journal***, Vol. 40, No. 7, (2002), 1444-1450.
17. Najafizadeh, M. and Heydari, H., "Thermal buckling of functionally graded circular plates based on higher order shear deformation plate theory", ***European Journal of Mechanics-A/Solids***, Vol. 23, No. 6, (2004), 1085-1100.
18. Najafizadeh, M. and Heydari, H., "An exact solution for buckling of functionally graded circular plates based on higher order shear deformation plate theory under uniform radial compression", ***International Journal of Mechanical Sciences***, Vol. 50, No. 3, (2008), 603-612.
19. Saidi, A., Rasouli, A. and Sahraee, S., "Axisymmetric bending and buckling analysis of thick functionally graded circular plates using unconstrained third-order shear deformation plate theory", ***Composite Structures***, Vol. 89, No. 1, (2009), 110-119.
20. Naderi, A. and Saidi, A., "Buckling analysis of functionally graded annular sector plates resting on elastic foundations", ***Proceedings of the Institution of Mechanical Engineers, Part C: Journal of Mechanical Engineering Science***, Vol. 225, No. 2, (2011), 312-325.
21. Naderi, A. and Saidi, A., "An analytical solution for buckling of moderately thick functionally graded sector and annular sector plates", ***Archive of Applied Mechanics***, Vol. 81, No. 6, (2011), 809-828.
22. Naderi, A. and Saidi, A., "Exact solution for stability analysis of moderately thick functionally graded sector plates on elastic foundation", ***Composite Structures***, Vol. 93, No. 2, (2011), 629-638.
23. Saidi, A. and Hasani Baferani, A., "Thermal buckling analysis of moderately thick functionally graded annular sector plates", ***Composite Structures***, Vol. 92, No. 7, (2010), 1744-1752.
24. Reddy, J. N., "Energy principles and variational methods in applied mechanics", Wiley New York, (2002).
25. Reddy, J. N., "Theory and analysis of elastic plates and shells", CRC, (2006).
26. Brush, D. O. and Almroth, B. O., "Buckling of bars, plates, and shells", McGraw-Hill New York, Vol. 6, (1975).
27. Wang, C., Wang, C. Y. and Reddy, J. N., "Exact solutions for buckling of structural members", CRC, Vol. 6, (2004).

On Symmetric and Asymmetric Buckling Modes of Functionally Graded Annular Plates under Mechanical and Thermal Loads

A. Hasani Baferani[a], A. R. Saidi [b], A. Naderi [b]

[a] *Department of Mechanical Engineering, Amirkabir University of Technology, Tehran, Iran.*
[b] *Department of Mechanical Engineering, Shahid Bahonar University of Kerman, Kerman, Iran.*

P A P E R I N F O

Paper history:
Received 29 December 2011
Received in revised form 03 October 2012
Accepted 18 October 2012

Keywords:
Annular Plate
Functionally Graded Material
Buckling
Thermal Buckling
Symmetric and Asymmetric Modes

چکیده

در این مقاله، کمانش حرارتی و مکانیکی ورق های نازک و نیمه ضخیم حلقوی ساخته شده از مواد هدفمند ارائه می شود. معادلات تعادل و پایداری ورق، بر اساس هر دو تئوری کلاسیک و برشی مرتبه اول ارائه شده است. معادلات وابسته خمشی و کششی پایداری ورق به دو معادله ی دیفرانسیلی مستقل ساده شده و در ادامه با حل معادلات دیفرانسیل مستقل حاکم و ارضای شرایط مرزی، مقدار بار و دمای بحرانی کمانش ارائه شده است. البته این نکته قابل ذکر است که در این مقاله حل متقارن محوری و غیرمتقارن محوری ورق حلقوی ساخته شده از مواد هدفمند در نظر گرفته شده است. بر اساس نتایج بدست آمده، میتوان دریافت که شماره ی مودهای کمانش با تغییرات توان ماده ی هدفمند، نسبت شعاع ها و نسبت شعاع به ضخامت تغییر میکند. در بخش نتایج عددی، اثر شعاع داخلی ورق، ضخامت ورق و توان ماده ی هدفمند بر کمانش حرارتی و مکانیکی ورق های حلقوی ساخته شده از مواد هدفمند ارائه شده است. در ضمن شکل مود کمانشی ورق حلقوی در یک وضعیت خاص ارائه شده است.

doi: *10.5829/idosi.ije.2013.26.04a.12*